VNU Journal of Science: Mathematics - Physics

Journal homepage: https://js.vnu.edu.vn/MaP

Original Article

Critical Behavior of a Correlated Impurity on Graphene

Dang The Hung[1,2,*], Nguyen Duc Tung[3], Luong Minh Tuan[3], Nguyen Hoang Linh[4], Dao Xuan Viet[3], Nghiem Thi Minh Hoa[2]

[1]*Phenikaa University, Yen Nghia, Ha Dong, Hanoi, Vietnam*

[2]*Phenikaa Institute for Advanced Study, Phenikaa University, Yen Nghia, Ha Dong, Hanoi, Vietnam*

[3]*Advanced Institute for Science and Technology, Hanoi University of Science and Technology, 40 Ta Quang Buu, Hanoi, Vietnam*

[4]*School of Engineering Physics, Hanoi University of Science and Technology, 1 Dai Co Viet, Hanoi, Vietnam*

Received 09 September 2021
Revised 09 October 2021; Accepted 09 October 2021

Abstract: The single-orbital Anderson impurity model using graphene as the host material is considered for the case where the impurity is placed on top of a carbon atom of the graphene lattice. This is an excellent setup for the $r = 1$ pseudogap impurity model, where there exists a quantum phase transition from the free local moment phase to the Kondo screening phase. In this work, the scaling behavior of the spin-spin correlator at quantum critical points is numerically investigated. It shows signatures of the logarithmic correction to scaling to the lowest temperature in use. Furthermore, the result suggests that the scaling dimension might vanish as $T \to 0$, thus the widely-accepted scaling behavior for $r < 1$ might be destroyed at $r = 1$, signifying that $r = 1$ is the upper critical dimension for the class of pseudogap impurity problem.

Keywords: Kondo model, Anderson impurity model, pseudogap, graphene, heavy fermion systems.

1. Introduction

The field of quantum phase transition and quantum critical points [1] is an active topic in modern condensed matter physics. It possesses a variety of challenging problems, especially in strongly

* Corresponding author.
E-mail address: hung.dangthe@phenikaa-uni.edu.vn

https//doi.org/10.25073/2588-1124/vnumap.4677

correlated systems. The reason is that it requires extreme conditions, in particular $T \to 0$, in order to observe the transition, and the quantum fluctuations, which control the phase transition, are not easily treated when due to correlated effects. The pioneering works of Hertz [2] and Millis [3] are the foundation of the conventional theory for quantum critical points. It is based on the Landau-Ginzburg paradigm for phase transitions, where the order parameter strongly fluctuates at long wavelength and dominates the physics at criticality. Furthermore, the system exhibits only Fermi liquid behavior in all phases. The Hertz-Millis theory has successfully explained the magnetic phase transitions in itinerant fermion systems and is considered as the foundation for quantum critical phenomena.

However, there are classes of materials, including heavy fermion metals and unconventional superconductors [4-6], which exhibit non Fermi liquid behaviors at criticality and cannot be described using the conventional theory. Going beyond the Landau-Ginzburg paradigm, Senthil et al [7] have proposed the concept "deconfined quantum critical points" where the quasiparticles representing the order parameter fluctuations exhibit fractional quantum numbers, thus being "deconfined" at criticality. Another approach for heavy fermion metals from Si et al [8] and Paschen et al [9] suggest that the phase transition between the antiferromagnetic and the paramagnetic phases, which is due to the competition between the Kondo scale and the Ruderman–Kittel–Kasuya–Yosida (RKKY) interaction in these systems [10], can be explained in terms of local quantum phase transitions at each site of the lattice. In these heavy fermion systems, the valence f electrons are rather localized and form a large local moment at each site, in resemblance to a Kondo impurity spin, which can be destroyed by tuning internal parameters, resulting in a local quantum critical point. This is the Kondo destruction phenomenon [8, 11, 12], which can be a leading factor to control the global quantum phase transition in heavy fermion systems.

Normally, there is no such quantum critical point in the standard Kondo impurity model [13]. However, the environments around each site in many heavy fermion systems resemble to a host material where the density of states (DOS) vanishes at the Fermi level following a power law of frequency $\nu(\omega) \sim |\omega|^r$. This problem can be simplified and described by a pseudogap Kondo model or (more generally) Anderson impurity model, which has been investigated intensively since the 1990s [14, 15, 16]. In this model, the Kondo screening effect does not always exist even at the symmetric case (one electron in average in the impurity). Depending on r, the phase transition from the free local moment phase to the Kondo screening phase can be observed by changing the Kondo coupling ($r < 1/2$) or by further valence mixing in addition to large Kondo coupling ($r > 1/2$) [16]. Therefore, to understand the physics of heavy fermion systems, one can in turns study the local quantum critical points in the corresponding pseudogap model, which thus leads to the resurgence of the research in pseudogap Kondo model in the 2010s [11, 12, 17-19].

Motivated by these studies, in this work, we focus on a case of the pseudogap Anderson model where the DOS of the host material is linear around the Fermi level ($r = 1$ case). This is a special case. In the theoretical aspect, $r = 1$ is the "upper critical dimension" in analogy to the concept in critical field theory [20, 21]. At this critical dimension, logarithmic corrections exist in many kinds of scaling [22] and above it the problem can be treated by an appropriate perturbative approach. In the experimental aspect, $r = 1$ case can be used to depict d-wave superconductors or heavy fermion systems, and recently the emergence of graphene [23] with its linear dispersion relation around the charge neutral point [24] makes this 2D material a prominent candidate for the realization of the $r = 1$ pseudogap model [17]. In this work, we focus on the physics of an impurity on graphene at the quantum critical point. In particular, we investigate the scaling functions of several physical observations by numerical simulations, calculating the corresponding critical exponents and comparing with previous studies for $r < 1$. We also discuss the effect of the logarithmic correction to scaling that affects our results. We expect to gain

more insights into the quantum critical phenomena that might occur in heavy fermion systems as well as in graphene lattice.

2. Formalism

We construct the Anderson impurity model [25] for the problem in which the impurity is a single-orbital one with at most two electrons for both spin up and spin down. The host material is assumed to be a honeycomb lattice, with only nearest neighbor hopping, which is already enough to simulate the low-energy band structure of graphene. Impurity electrons are allowed to hybridize only between the impurity and the nearest lattice sites. In general, the position of the impurity plays an important role in this hybridization, thus affecting the local physics of the impurity. However, in this work, we assume that the impurity position is on top of a site in the honeycomb lattice, which results in the hybridization function only different from the DOS of the graphene lattice by a prefactor [26]. The use of graphene as the host material is two-fold. First, it allows for direct testing the possibility to realize the pseudogap Kondo physics on graphene. Second, our previous work [26] showed that for impurity on top of a carbon of the graphene lattice, the results are rather similar to those of the conventional pseudogap impurity model [16] at $r = 1$, thus the results presented in this work can be also applied to $r = 1$ case.

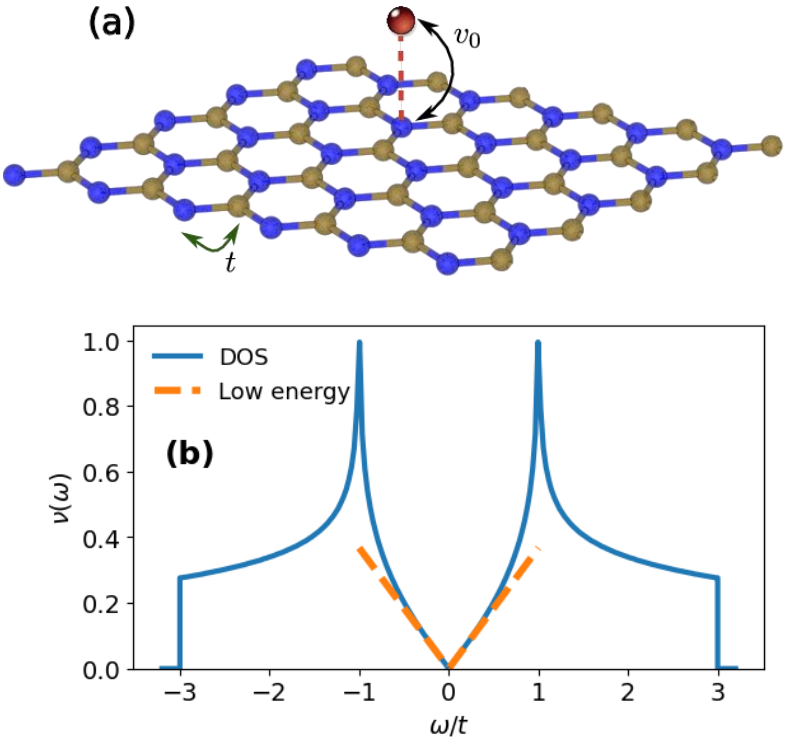

Figure 1. (a) Illustration of a single-orbital impurity placed on top of a carbon atom of the graphene lattice. Electrons hop between the impurity and the site underneath with a hopping amplitude v_0. On graphene, conduction electrons hop between nearest neighbor sites with an amplitude t. Different colors of lattice sites mark different sublattices. (b) The density of states (DOS) of graphene lattice when there is only the nearest neighbor hopping t. The dashed line exhibits the low-energy linear behavior of the DOS.

Following the above description, the Hamiltonian of this model is composed of three parts [26] which can be constructed in real space. The kinetic Hamiltonian of the host is written in the tight-binding form with only the nearest neighbor hopping t:

$$H_{host} = -t \sum_{i\alpha,j\beta,\sigma} c^{\dagger}_{i\alpha\sigma} c_{j\beta\sigma}. \tag{1}$$

The local Hamiltonian of the impurity expresses the Anderson impurity model:

$$H_{imp} = \epsilon_d (n_{d\uparrow} + n_{d\downarrow}) + U n_{d\uparrow} n_{d\downarrow}. \tag{2}$$

Lastly, the hybridization part is also constructed using the tight-binding approach where the nearest neighbor hybridization is v_0 (assuming the impurity is placed on top of a site belonging to sublattice A of graphene lattice):

$$H_{hyb} = v_0 \sum_{i\sigma} d^{\dagger}_{\sigma} c_{iA\sigma} + c^{\dagger}_{iA\sigma} d_{\sigma}. \tag{3}$$

In these expressions, $c^{\dagger}_{i\alpha\sigma}, c_{j\beta\sigma}$ ($d^{\dagger}_{\sigma}, d_{\sigma}$) are the creation and annihilation operators of the graphene lattice (impurity), respectively. n_{σ} is the impurity occupancy operator for spin σ: $n_{\sigma} = d^{\dagger}_{\sigma} d_{\sigma}$. The notation α, β are graphene sublattice indices ($\alpha, \beta = A, B$), σ is the spin index. The impurity Hamiltonian has two parameters: the impurity energy level ϵ_d and the Hubbard interaction strength U. In this model, there are 5 parameters in total: v_0, t, U and ϵ_d together with the temperature T. However, t is normally used as basic energy scale and is kept fixed, and $1/T$ is treated as the "system size" for finite-size scaling analysis [11, 12]. Thus there are only 3 parameters left (U, ϵ_d and v_0) for varying.

Throughout this work, we employ the hybridization expansion continuous-time Quantum Monte Carlo method (CT-HYB) [27-29] to treat the model, which is implemented in the TRIQS package [30, 31]. CT-HYB is a nonzero-temperature method which can solve the model numerically exactly and has been proved to work rather well with pseudogap Anderson impurity models [11, 12, 26]. Compared with the numerical renormalization group (NRG) method [32], the disadvantages of the CT-HYB is that it is unable to go to low-temperature regime and is computationally demanding. However, the advantages is that the setup to solve the pseudogap model with CT-HYB is rather straightforward and measuring dynamical quantities are feasible, thus allowing for the scaling analysis, which is the main focus of our work.

Normally, dynamical quantities can be represented by correlation functions. Given an operator of a physical observable $\hat{\phi}$, the corresponding correlation function in imaginary time is:

$$C_{\phi}(\tau) = \langle T\phi(\tau)\phi(0)\rangle, \tag{4}$$

where T is the time-order operator and τ is the imaginary time. This function tells how ϕ at the times τ and 0 are related to each other. By analytical continuation to real frequency, it results in the spectral function of excitations related to the physical observable ϕ, implying how ϕ is changed by external field that is coupled to ϕ. In this work, we focus on the scaling behavior of the spin-spin correlator in the impurity. The form of this correlator is:

$$C_s(\tau) = \langle \sigma_z(\tau)\sigma_z(0)\rangle, \tag{5}$$

where σ_z is the z component of the spin-1/2 operator ($\sigma_z = n_{d\uparrow} - n_{d\downarrow}$). The right expression in Formula (5) is averaged by Monte Carlo measurements. To avoid artificial spin polarization in the simulation, especially at low temperature, global update by swapping operators of spin up and down is enabled in the simulation. A typical simulation is carried out with at least 10^8 Monte Carlo measurements, where there are 200 Monte Carlo updates between two consecutive measurements, in

order to measure 30 τ-points of the correlator $C_s(\tau)$. Finer calculation is carried out with similar number of Monte Carlo measurements but with 500 τ-points of the correlator.

The impurity spin susceptibility, which explicitly tells how the impurity local moment resists to the external magnetic field, is obtained from the spin-spin correlation function:

$$\chi_s = \int_0^\beta \langle \sigma_z(\tau)\sigma_z(0)d\tau. \tag{6}$$

The spin-spin correlation function and the spin susceptibility (as well as other quantities such as charge susceptibility and charge correlation function, etc.) are important when studying critical phenomena. At criticality, such correlation functions at different temperatures usually collapse when rescaling the imaginary time appropriately, while the susceptibilities can be written as power laws of temperature. In particular, for the spin operator, the spin-spin correlation function is scaled as [37, 42]:

$$\langle \phi(\tau)\phi(0)\rangle = C\left(\frac{\pi T}{\sin(\pi\tau T)}\right)^{2\Delta}, \tag{7}$$

while the spin susceptibility depends on the temperature as [18, 42]:

$$\chi_s(T) \sim T^{-x_s}. \tag{8}$$

Δ and x_s are so-called critical exponents for this impurity problem. Furthermore, Δ plays a similar role as the dimension in the classical field theory, it is named the scaling dimension. In similarity to classical field theory, there are hyperscaling relations involving the dimension and critical exponents, in this case it is the relation between Δ and x_s [42]:

$$2\Delta + x_s = 1. \tag{9}$$

3. Results

As described in Section 2, we consider the scenario of an impurity placed on top of a carbon atom in the graphene lattice (the t site) [see Fig. 1(a)]. At this position, the hybridization function [29, 3], which describes the dynamics of electrons hopping between the impurity and the host material, is only different from the DOS of graphene by a prefactor $v_0^2/2$ [26]. As the DOS of graphene is linear in frequency around the Fermi level [24] [see Fig. 1(b)], the impurity is aware of this linear relation directly from the hybridization function, thus making this scenario a perfect one to study the $r = 1$ pseudogap Kondo physics.

The first step for studying critical behavior of a system is to search for the critical points. For non-zero temperature method such as CT-HYB, the method of choice is to consider the inverse temperature $1/T$ as the "size" of the system and carry out Binder analysis [34] to extrapolate the critical point at $T = 0$ [11, 12]. We have applied this method successfully in our previous work to construct the full phase diagram of this model [26]. In this work, we extract the values of several critical points on the phase boundary from Ref. 26 for studying further the scaling behavior and critical exponents.

At criticality, boundary conformal field theory states that finite-temperature correlation functions in imaginary time follow a scaling form [35, 36, 37]

$$\langle \phi(\tau)\phi(0)\rangle = F\left(\frac{\pi T}{\sin(\pi\tau T)}\right) \tag{10}$$

In the long time regime ($0 \ll \tau \ll 1/T$), the scaling function becomes:

$$F\left(\frac{\pi T}{\sin(\pi\tau T)}\right) = C\left(\frac{\pi T}{\sin(\pi\tau T)}\right)^{2\Delta}, \tag{11}$$

where Δ is the scaling dimension, C is a constant prefactor and τ is the imaginary time running from 0 to $1/T$. If $2\Delta > 1$, the transformation from imaginary time to frequency in Eq. (11) does not converge. But more often, $0 < 2\Delta < 1$, Eq. (11) can be transformed into the Matsubara frequency form

$$C\int_0^{1/T} e^{i\omega_n\tau}\left(\frac{\pi T}{\sin(\pi\tau T)}\right)^{2\Delta} d\tau = \frac{2\sin(\Delta\pi)}{(2\pi T)^{1-2\Delta}} B(\Delta+n, 1-2\Delta), \tag{12}$$

where $B(x, y)$ is the beta function and $\omega_n = 2n\pi T$ with an integer n is the Matsubara frequency for bosons. The real frequency correlation function is obtained by analytic continuation (replacing $i\omega_n$ by $\omega + i0^+$), thus the result from Ref. 37 is reproduced

$$(2\pi T)^{1-2\Delta}\langle\phi(\tau)\phi(0)\rangle = 2B\left(\Delta - \frac{i}{2\pi}\frac{\omega}{T}, 1-2\Delta\right)\sin(\Delta\pi), \tag{13}$$

which exhibits the ω/T scaling form, as observed in the magnetic susceptibility of several heavy fermion systems [38, 39, 40, 41]. The experimental data for ω/T scaling form provides crucial evidence for the non-Fermi liquid behavior in these materials, distinguishing it from the conventional Hertz-Millis theory. From the theoretical aspect, this scaling form is observed in pseudogap impurity models at $r < 1$ [11, 12, 42], leading to the statement by Si and coworkers [8, 9, 43] that QCPs occur in heavy fermion metals are likely due to the local QCPs at each site of the lattice.

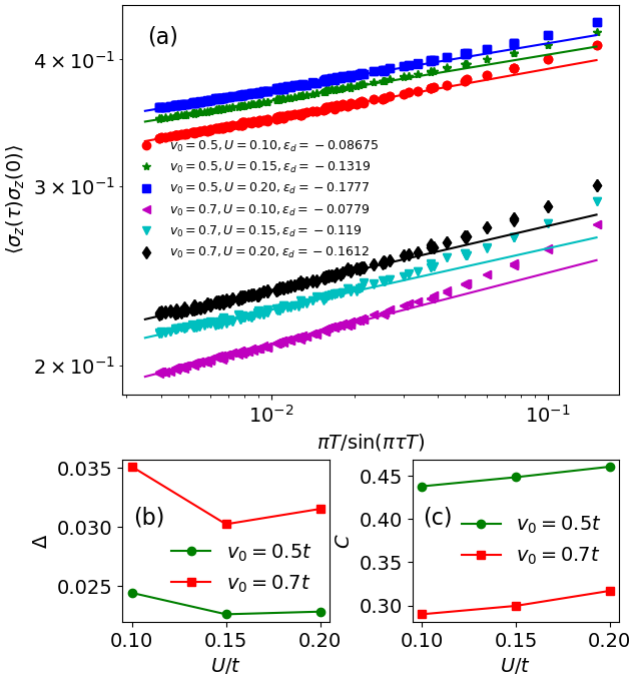

Figure 2. (a) The dependence of the spin-spin correlator on $\pi T/\sin(\pi\tau T)$ at six different QCPs plotted in the logarithmic scale. Each curve of (v_0, U) is composed of data of 7 different temperatures (using the same color) ranging from $t/800$ to $t/200$. The solid line for each case is the linear fit at small $\pi T/\sin(\pi\tau T)$. (b) The critical exponent Δ in Eq. (10) plotted with respect to U. (c) The prefactor C in Eq. (10) vs. U.

We investigate this scaling behavior for the $r = 1$ pseudogap impurity model by measuring the spin-spin correlator $C_s(\tau) = \langle T\sigma_z(\tau)\sigma_z(0)\rangle$. Figure 2(a) shows six different cases of (v_0, U) where $v_0 = 0.5t, 0.7t$ and $U = 0.1t, 0.15t, 0.2t$. For each case, when plotting $C_s(\tau)$ vs. $\pi T/\sin(\pi\tau T)$, data points of all temperatures in use (T runs from $t/800$ to $t/200$) collapse into a single curve for nearly two decades, confirming the scaling form in Eq. (10). This results are rather well understood since $\pi T/\sin(\pi\tau T)$ scaling is ubiquitous for systems with conformal invariance [35]. However, to ensure the ω/T scaling, one needs to show that $C_s(\tau)$ exhibits the scaling form in Eq. (11) with $2\Delta < 1$. For that reason, we conduct linear fit for the curves in Fig. 2(a) for large τ (the fitting range is $\pi T/\sin(\pi\tau T) < 2 \times 10^{-2}t$), which exhibits the scaling form as in Eq. (11) at large τ. The prefactor C extracted from the linear fit as plotted in Fig. 2(c) is directly proportional to U, which is understandable as larger correlation means the local moment is more rigid to rotate, thus the spin-spin correlation is increased with respect to U. At small $v_0 = 0.5t$, the local moment gets even more localized, the C values are 50% larger than that at $v_0 = 0.7t$.

However, the critical exponent Δ is unexpected. First, we notice that $\Delta \sim 0.022$ for $v_0 = 0.5t$ and ~ 0.032 for $v_0 = 0.7t$, which are much smaller than those at small r ($\Delta = 0.10$ at $r = 0.6$ [12] and 0.16 at $r = 0.4$ [11]). Second, more importantly, the values of the critical exponent Δ for six different cases of (v_0, U) are not the same. The value of Δ at $v_0 = 0.7$ is about 40% larger than that of $v_0 = 0.5$ which is beyond the error bar. It is a crucial issue because the scaling form is universal and thus Δ should be the same even for different U or v_0. One reason for this difference is that the temperature in use for CT-HYB simulations is not low enough, thus $C_s(\tau)$ still contains large curvature that causes fitting error for the critical exponent. But a more important reason is that the logarithmic correction to scaling at $r = 1$ [22] may appear in the scaling form in Eq. (11) for the whole range of temperature, which may affect the scaling form at different magnitude depending on how strong the correlation is.

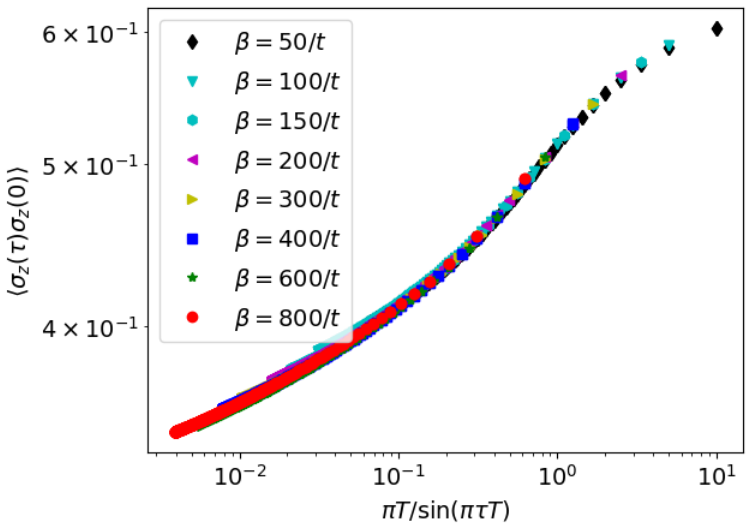

Figure 3. The spin-spin correlator vs. $\pi T/\sin(\pi\tau T)$ at the critical point at $U = 0.15t$, $v_0 = 0.5t$ with a fine grid of 500 τ-points for each temperature. The inverse temperature is $\beta = 1/T$.

We focus more on this logarithmic correction to scaling. The signature of this correction in Fig. 2(a) is the curvature from the straight line at small τ (i.e. large $\pi T/\sin(\pi\tau T)$), which we believe does not disappear for nonzero temperatures. Normally, for $r < 1$, the scaling form in Eq. (11) approaches the

power-law behavior (or linear behavior in the logarithmic scale) rather quickly before the bending of the curve at $\tau \sim 0$ (or $\tau \sim \beta$) [11, 12, 37]. But the scaling form at $r = 1$ does not behave in this way, it tends to rise above the fitting line at low τ, showing opposite curvature as compared with $r < 1$ cases. To understand further, we plot in Figure 3 the calculation at a specific critical point ($U = 0.15t$ and $v_0 = 0.5t$) using a much finer τ grid with 500 points (10 times denser) while maintaining the number of Monte Carlo measurements unchanged or even larger than those producing Fig. 2. With such a finer grid, Fig. 3 shows the bending at x axis value $\gtrsim 1$, similar to those for $r < 1$ cases [11, 12, 37]. Moreover, this figure shows that there is curvature at smaller $\pi T/\sin(\pi\tau T)$ (~ 0.4), and tends to exist even at lower temperatures. (In Fig. 3, the lowest-temperature curve ($\beta = 800/t$) still exhibits curvature at its lowest x value.) Thus we believe that Fig. 3 provides certain evidence that there is logarithmic correction to scaling which may ruin the scaling behavior.

Consequently, it poses a problem that the scaling dimension Δ may not be calculated correctly, and furthermore, the scaling form in Eq. (11) may not exist in the case $r = 1$. It means that the susceptibility (and other dynamical quantities) may not have the ω/T scaling form that is well observed for other cases at $r < 1$. We recall that the $r = 1$ case is considered as the "upper critical dimension" [20, 21]. At $r = 1$, logarithmic correction to scaling exists [22], below $r = 1$, the system exhibits nontrivial fixed points and well-defined scaling behavior (such as ω/T scaling), while above $r = 1$, such scaling behavior is violated and the problem can be treated with perturbative corrections. Therefore, it is not surprising for odd characteristics in the scaling analysis of $r = 1$ case. As the logarithmic correction to scaling exists in the problem, one thus hardly achieves the scaling as in Eq. (11) regardless of how low the temperature is.

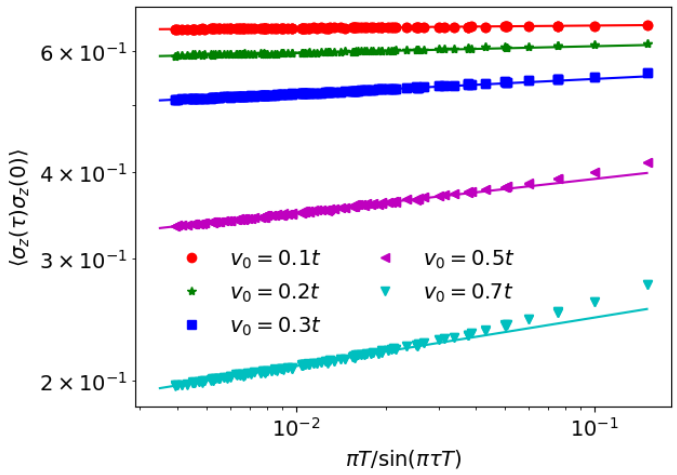

Figure 4. The spin-spin correlator vs. $\pi T/\sin(\pi\tau T)$ at criticality for several values of v_0 at fixed $U = 0.1t$.

To gain further insights into this issue, we plot in Figure 4 the scaling form of $C_s(\tau)$ at different v_0 values. The reason is that the correlation strength depends much more on v_0 than U, one can then easily see how well the scaling form exhibits at finite temperatures when the correlation strength largely changes. Normally, the correlation strength increases significantly at small v_0 (assuming other parameters are unchanged), which means the smaller v_0, the lower temperature required to observe the power-law behavior of $C_s(\tau)$, which applies to $r < 1$ cases. Therefore, for $r < 1$, the scaling dimension Δ can be obtained more easily at larger v_0, while for small v_0, it requires lower temperature so that the system asymptotically approaches the universal scaling form. However, the case $r = 1$ behaves in an opposite way. Fig. 4 shows that at large v_0, the linear fit is improved as v_0 decreases. It is known that

when there is no hybridization between the impurity and the host material ($v_0 = 0$), there is no such a scaling as in Eq. (10), thus $\Delta = 0$. At a fixed temperature, as v_0 decreases, Δ obtained from the linear fitting also decreases. If Δ is nonzero (as for $r < 1$ cases), for each v_0, there is a corresponding temperature scale T_Δ, below which the linear fit gives correct value of Δ. This T_Δ decreases exponentially with respect to v_0, thus at $r < 1$, the fitting at small v_0 does not work well. However, at $r = 1$, the goodness of fit turns out to be better for small v_0, which only happens if $\Delta = 0$. Thus this unusual characteristic of the scaling at $r = 1$ suggests that the scaling dimension Δ should vanish.

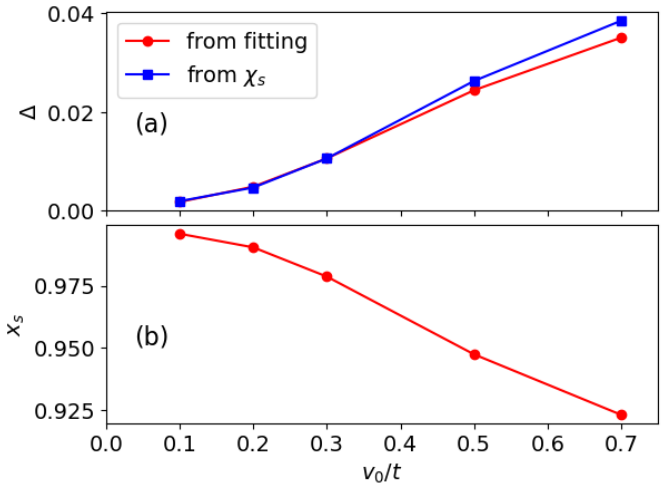

Figure 5. (a) The scaling dimension Δ as a function of v_0 calculated in two ways: (1) extracted directly from the spin-spin correlator $C_s(\tau)$ (red circle), (2) derived using the hyperscaling relation $x_s = 1 - 2\Delta$. (b) Critical exponents for charge and spin local susceptibilities as a function of v_0.

We further check our statement by estimating the critical exponent x_s of the impurity spin susceptibility χ_s as introduced in Sec. 2. At low temperatures, the impurity spin susceptibility has an asymptotic power law of temperature [42]

$$\chi_s(T) \sim T^{-x_s}. \tag{14}$$

Because of the hyperscaling relation $2\Delta + x_s = 1$, we can derive Δ from χ_s to check our results above. Figure 5 shows χ_s and Δ as functions of v_0. Δ values obtained in two ways coincide at $v_0 < 0.3t$, while at $v > 0.3t$, there are clear differences between the two ways of calculations. Thus Fig. 5 is another evidence that $C_s(\tau)$ may reach its asymptotic behavior at higher T when v_0 is smaller.

Considering previous works in this topic, attempts to calculate the critical charge or spin exponent $x_{c,s}$ have been conducted for a wide range of r [18, 42]. Their results show that $x_{c,s}$ both approach unity as $r \to 1$, specifically, $x_c \approx 0.8$ [18] and $x_s \approx 0.93$ [42] for $r = 0.9$. It is therefore consistent with our result that x_s tends to go towards unity (or Δ might vanish) at $r = 1$. Thus if Δ indeed vanishes, we can describe the evolution of the scaling behavior as T decreases to zero. At high temperature, by fitting the scaling curve, Δ is significantly nonzero ($\sim 0.2, \sim 0.3$ for $v_0 = 0.5t, 0.7t$, respectively). However, due to the logarithmic correction to scaling, there is always convex curvature in the scaling curve $C_s(\tau)$ at any temperature. As T decreases, the fitting line becomes closer to the horizontal line, which means as $T \to 0$, $\Delta \to 0$. It means the scaling behavior at $r < 1$ is destroyed, which is a crucial signature for the "upper critical dimension" at $r = 1$.

4. Conclusion

In this work, we have conducted rigorous numerical calculations to investigate the scaling behavior of the spin-spin correlator $C_s(\tau)$ for the $r = 1$ pseudogap Anderson impurity model, of which the host material is a honeycomb lattice, simulating graphene. We calculated the spin-spin correlators at critical points, which are highly demanding numerical simulations with the CT-HYB method. We observed the scaling form $F(\pi T/\sin(\pi\tau T)$ as predicted by the boundary conformal field theory. We considered this scaling function as a power law of $\pi T/\sin(\pi\tau T)$ and estimated the exponent Δ of this power law, which is the scaling dimension of the model. We justified our estimation by showing that the hyperscaling relation for Δ and the critical exponent of the spin susceptibility is satisfied. We also investigated carefully the scaling behavior of the spin-spin correlator and showed that there might exist convex curvature in the scaling form at large τ region even at low temperature, which is attributed to the logarithmic correction to scaling that exists specifically in the $r = 1$ case. Moreover, we observed that $C_s(\tau)$ goes to the asymptotic scaling form faster when the correlation strength is larger, in opposite way as in $r < 1$ cases, and based on this behavior concluded that the scaling dimension Δ vanishes for the $r = 1$ pseudogap impurity model.

Our study contains several important findings. First, our scaling analysis shows certain convex curvature even at the lowest temperature, which is different from previous works, implying the logarithmic correction to scaling that occurs only in the $r = 1$ case. More importantly, our statement that Δ, which may be unable to calculate at finite temperature, approaches 0 as $T \to 0$. It means that at criticality, the impurity local moment behaves as if it were a completely free moment, without any hybridization with the host material. Vanishing Δ also signifies the fact that $r = 1$ is indeed an upper critical dimension. For $r < 1$, there is a well-defined scaling form of dynamical quantities. At $r = 1$, the scaling dimension vanishes, implying scaling behavior is destroyed at $r \geq 1$.

We propose further direction in this research topic. A prospective future direction could be using the numerical renormalization group (NRG) method, which is capable of accessing extremely low-temperature regime. Although there are difficulties in calculating dynamical quantities in NRG, one can instead calculate the critical exponent of the susceptibility and employ the hyperscaling relation to derive the scaling dimension Δ, providing a potential approach to assess our statement in this work. From the experimental aspect, one can suggest that graphene could be an interesting material to examine the pseudogap model at critical dimension. If one can pin down the impurity on top of a carbon atom, measurements of frequency-dependent susceptibility or impurity spectral function may show interesting scaling behavior that only exists at critical dimension.

Acknowledgments

This research is funded by Vietnam National Foundation for Science and Technology Development (NAFOSTED) under grant number 103.01-2018.12. We also acknowledge the support for the allocation of computing time at Jülich Supercomputing Centre. Portion of our calculation as well as data post-processing tasks has been performed using the computer cluster of Phenikaa Institute for Advanced Study.

References

[1] S. Sachdev, Quantum Phase Transitions second edition, Cambridge University Press, Cambridge, 2011.
[2] J. A. Hertz, Quantum Critical Phenomena, Physical Review B, Vol. 14, 1976, pp. 1165-1184, https://doi.org/10.1103/PhysRevB.14.1165.

[3] A. J. Millis, Effect of a Nonzero Temperature on Quantum Critical Points in Itinerant Fermion Systems, Physical Review B, Vol. 48, 1993, pp. 7183-7196, https://doi.org/10.1103/PhysRevB.48.7183.
[4] H. V. Löhneysen, T. Pietrus, G. Portisch, H. G. Schlager, A. Schröder, M. Sieck, and T. Trappmann, Non-Fermi-Liquid Behavior in a Heavy-Fermion Alloy at a Magnetic Instability, Physical Review Letters, Vol. 72, 1994, pp. 3262-3265, https://doi.org/10.1103/PhysRevLett.72.3262.
[5] G. R. Stewart, Non-Fermi-Liquid Behavior in d- and f-electron Metals, Reviews of Modern Physics, Vol. 73, 2001, pp. 797-855, https://doi.org/10.1103/RevModPhys.73.797.
[6] P. Gegenwart, Q. Si, F. Steglich, Quantum Criticality in Heavy-Fermion Metals, Nature Physics, Vol. 4, 2008, pp. 186-197, https://doi.org/10.1038/nphys892.
[7] T. Senthil, Deconfined Quantum Critical Points, Science, Vol. 303, 2004, pp. 1490-1494, https://doi.org/10.1126/science.1091806.
[8] Q. Si, S. Rabello, K. Ingersent, J. L. Smith, Locally Critical Quantum Phase Transitions in Strongly Correlated Metals, Nature, Vol. 413, 2001, pp. 804-808, https://doi.org/10.1038/35101507.
[9] S. Paschen, Q. Si, Quantum Phases Driven by Strong Correlations, Nature Reviews Physics, Vol. 3, 2021, pp. 9-26, https://doi.org/10.1038/s42254-020-00262-6.
[10] S. Doniach, The Kondo Lattice and Weak Antiferromagnetism, Physica B+C, Vol. 91, 1977, pp. 231-234, https://doi.org/10.1016/0378-4363(77)90190-5.
[11] M. T. Glossop, S. Kirchner, J. H. Pixley, Q. Si, Critical Kondo Destruction in a Pseudogap Anderson Model: Scaling and Relaxational Dynamics, Physical Review Letters, Vol. 107, 2011, pp. 076404, https://doi.org/10.1103/PhysRevLett.107.076404.
[12] J. H. Pixley, Stefan Kirchner, Kevin Ingersent, and Qimiao Si, Kondo Destruction and Valence Fluctuations in an Anderson Model, Physical Review Letters, Vol. 109, 2012, pp. 086403, https://doi.org/10.1103/PhysRevLett.109.086403.
[13] Alexander Cyril Hewson, The Kondo Problem to Heavy Fermions, Cambridge University Press, Cambridge, UK, 1993.
[14] D. Withoff, E. Fradkin, Phase Transitions in Gapless Fermi Systems with Magnetic Impurities, Physical Review Letters, Vol. 64, 1990, pp. 1835-1838, https://doi.org/10.1103/PhysRevLett.64.1835.
[15] R. Bulla, T. Pruschke, A. C. Hewson, Anderson Impurity in Pseudo-Gap Fermi Systems, Journal of Physics: Condensed Matter, Vol. 9, 1997, pp. 10463-10474, https://doi.org/10.1088/0953-8984/9/47/014.
[16] C. G. Buxton, K. Ingersent, Renormalization-Group Study of Anderson and Kondo Impurities in Gapless Fermi Systems, Physical Review B, Vol. 57, 1998, pp. 14254-14293, https://doi.org/10.1103/PhysRevB.57.14254.
[17] L. Fritz, M. Vojta, The Physics of Kondo Impurities in Graphene, Reports on Progress in Physics, Vol. 76, 2013, pp. 032501, https://doi.org/10.1088/0034-4885/76/3/032501.
[18] Tathagata Chowdhury and Kevin Ingersent, Critical Charge Fluctuations in a Pseudogap Anderson Model, Physical Review B, Vol. 91, 2015, pp. 035118, https://doi.org/10.1103/PhysRevB.91.035118.
[19] C. Wagner, T. Chowdhury, J. H. Pixley, K.Ingersent, Long-Range Entanglement near a Kondo-Destruction Quantum Critical Point, Physical Review Letters, Vol. 121, 2018, pp. 147602, https://doi.org/10.1103/PhysRevLett.121.147602.
[20] M. Vojta, L. Fritz, Upper Critical Dimension in A Quantum Impurity Model: Critical Theory Of The Asymmetric Pseudogap Kondo Problem, Physical Review B, Vol. 70, 2004, pp. 094502, https://doi.org/10.1103/PhysRevB.70.094502.
[21] L. Fritz, M. Vojta, Phase Transitions in The Pseudogap Anderson and Kondo Models: Critical Dimensions, Renormalization Group, and Local-Moment Criticality, Physical Review B, Vol. 70, 2004, pp. 214427, https://doi.org/10.1103/PhysRevB.70.214427.
[22] C. R. Cassanello, E. Fradkin, Kondo Effect in Flux Phases, Physical Review B, Vol. 53, 1996, pp. 15079–15094.
[23] K. S. Novoselov, A. K. Geim, S. V. Morozov, D. Jiang, Y. Zhang, S. V. Dubonos, I. V. Grigorieva, A. A. Firsov, Electric Field Effect in Atomically Thin Carbon Films, Science, Vol. 306, 2004, pp. 666-669, https://doi.org/10.1126/science.1102896.
[24] A. H. C. Neto, N. M. R. Peres, K. S. Novoselov, A. K. Geim, The Electronic Properties of Graphene. Rev. Mod. Phys., Vol. 81, 2009, pp. 109-162, https://doi.org/10.1103/RevModPhys.81.109.
[25] P. W. Anderson, Localized Magnetic States in Metals. Physical Review, Vol. 124, 1961, pp. 41-53, https://doi.org/10.1103/PhysRev.124.41.
[26] H. T. Dang, N. T. M. Hoa, Phase Diagram of a Pseudogap Anderson Model with Application to Graphene, arXiv:2107.09854 [cond-mat], 2021, https://doi.org/10.48550/arXiv.2107.09854.

[27] Philipp Werner and Andrew J. Millis, Hybridization Expansion Impurity Solver: General Formulation and Application to Kondo Lattice and Two-Orbital Models, Physical Review B, Vol. 74, 2006, pp. 155107, https://doi.org/10.1103/PhysRevB.74.155107.
[28] P. Werner, A. Comanac, Luca de' Medici, Matthias Troyer, and Andrew J. Millis, Continuous-Time Solver for Quantum Impurity Models, Physical Review Letters, Vol. 97, 2006, pp. 076405, https://doi.org/10.1103/PhysRevLett.97.076405.
[29] E. Gull, A. J. Millis, A. I. Lichtenstein, A. N. Rubtsov, M. Troyer, P. Werner, Continuous-Time Monte Carlo Methods for Quantum Impurity Models, Reviews of Modern Physics, Vol. 83, 2011, pp. 349-404, https://doi.org/10.1103/RevModPhys.83.349.
[30] O. Parcollet, M. Ferrero, T. Ayral, H. Hafermann, I. Krivenko, L. Messio, P. Seth, TRIQS: A Toolbox for Research on Interacting Quantum Systems, Computer Physics Communications, Vol. 196, 2015, pp. 398-415, https://doi.org/10.1016/j.cpc.2015.04.023.
[31] P. Seth, I. Krivenko, M. Ferrero, O. Parcollet, TRIQS/CTHYB: A Continuous-Time Quantum Monte Carlo Hybridisation Expansion Solver for Quantum Impurity Problems. Computer Physics Communications, Vol. 200, 2016, pp. 274-284, https://doi.org/10.1016/j.cpc.2015.10.023.
[32] R.Bulla, T. A. Costi, T. Pruschke, Numerical Renormalization Group Method for Quantum Impurity Systems, Reviews of Modern Physics, Vol. 80, 2008, pp. 395-450, https://doi.org/10.1103/RevModPhys.80.395.
[33] A. Georges, G. Kotliar, W. Krauth, M. Rozenberg, Dynamical Mean-Field Theory of Strongly Correlated Fermion Systems and The Limit of Infinite Dimensions, Reviews of Modern Physics, Vol. 68, 1996, pp. 113-125, https://doi.org/10.1103/RevModPhys.68.13.
[34] K. Binder, Finite Size Scaling Analysis of Ising Model Block Distribution Functions, Zeitschrift für Physik B Condensed Matter, Vol. 43, 1981, pp. 119-140, https://doi.org/10.1007/BF01293604.
[35] J. L. Cardy, Conformal Invariance and Surface Critical Behavior, Nuclear Physics B, Vol. 240, 1984, pp. 514–532, https://doi.org/10.1016/0550-3213(84)90241-4.
[36] I. Affleck, A. W. W. Ludwig, Critical Theory of Overscreened Kondo Fixed Points, Nuclear Physics B, Vol. 360, 1991, pp. 641-696, https://doi.org/10.1016/0550-3213(91)90419-X.
[37] S. Kirchner, Q. Si, Scaling and Enhanced Symmetry at the Quantum Critical Point of the Sub-Ohmic Bose-Fermi Kondo Model, Physical Review Letters, Vol. 100, 2008, pp. 026403, https://doi.org/10.1103/PhysRevLett.100.026403.
[38] A. Schröder, G. Aeppli, E. Bucher, R. Ramazashvili, and P. Coleman, Scaling of Magnetic Fluctuations near a Quantum Phase Transition, Physical Review Letters, Vol. 80, 1998, pp. 5623-5626, https://doi.org/10.1103/PhysRevLett.80.5623.
[39] A. Schröder, G. Aeppli, R. Coldea, M. Adams, O. Stockert, H. v Löhneysen, E. Bucher, R. Ramazashvili, P. Coleman, Onset of Antiferromagnetism in Heavy-Fermion Metals, Nature, Vol. 407, 2000, pp. 351–355, https://doi.org/10.1038/35030039.
[40] M. C. Aronson, R. Osborn, R. A. Robinson, J. W. Lynn, R. Chau, C. L. Seaman, M. B. Maple, Non-Fermi-Liquid Scaling of the Magnetic Response in UCu {5 - X}Pd x (x=1,1.5), Physical Review Letters, Vol. 75, 1995, pp. 725-728, https://doi.org/10.1103/PhysRevLett.75.725.
[41] H. V. Löhneysen, A. Rosch, M. Vojta, P. Wölfle, Fermi-Liquid Instabilities at Magnetic Quantum Phase Transitions, Reviews of Modern Physics, Vol. 79, 2007, pp. 1015-1075, https://doi.org/10.1103/RevModPhys.79.1015.
[42] K. Ingersent, Q. Si, Critical Local-Moment Fluctuations, Anomalous Exponents, and ω / T Scaling in the Kondo Problem with a Pseudogap, Physical Review Letters, Vol. 89, 2002, pp. 076403, https://doi.org/10.1103/PhysRevLett.89.076403.
[43] Q. Si, F. Steglich, Heavy Fermions and Quantum Phase Transitions, Science, Vol. 329, 2010, pp. 1161, https://doi.org/10.1126/science.1191195.